

# Assembly and Stepwise Oxidation of Interpenetrated Coordination Cages Based on Phenothiazine\*\*

Marina Frank, Jakob Hey, Ilker Balcioglu, Yu-Sheng Chen, Dietmar Stalke, Tomoyoshi Suenobu, Shunichi Fukuzumi, Holm Frauendorf, and Guido H. Clever\*

Research on coordination cages<sup>[1]</sup> which self-assemble from organic ligands and metal ions is shifting more and more from a focus on structural aspects towards the implementation of function.<sup>[2]</sup> In this sense, coordination cages have found application in fields such as selective anion recognition,<sup>[3]</sup> sequestering of hazardous substances,<sup>[4]</sup> drug delivery,<sup>[5]</sup> stabilization of reactive reagents and intermediates,<sup>[6]</sup> catalysis,<sup>[7]</sup> material science, and photophysical devices.<sup>[8]</sup>

For the area of non-silicon photovoltaics<sup>[9]</sup> as well as for the related topic of molecular electronics,<sup>[10]</sup> discrete redox-active (in)organic compounds show potential for technological application<sup>[11]</sup> because of their tuneable optical and electronic properties, monodispersity, and bottom-up integration into complex aggregates of defined morphology.<sup>[12]</sup> The pharmaceutically important heterocycle phenothiazine (**1**)<sup>[13]</sup> serves as a promising candidate for the preparation of such materials because of its beneficial redox behavior of readily undergoing a reversible one-electron oxidation to its radical cation ( $E^0 = +0.73$  V in acetonitrile versus SCE)<sup>[14]</sup> with the possibility of further oxidation or disproportionation processes.<sup>[15]</sup> Consequently, monomeric phenothiazine species

have been widely used as electron-donor components in systems capable of photoinduced charge separation,<sup>[16]</sup> as charge carriers in light-powered molecular machines,<sup>[17]</sup> and as redox shuttles in lithium-ion batteries.<sup>[18]</sup> To enhance the electro- and photochemical properties and to be able to study cooperative phenomena, Müller and co-workers have prepared phenothiazine-based conjugated oligomers<sup>[19]</sup> and rings<sup>[20]</sup> by using a covalent approach based on C–C cross-coupling reactions.<sup>[21]</sup> Although this route was shown to deliver a variety of multimeric phenothiazine derivatives, it suffers from the typical material losses associated with multistep synthesis and the need for tedious purification protocols.

Research on the rational self-assembly of metal–organic architectures such as rings, cages,<sup>[1]</sup> and knots<sup>[22]</sup> has shown, however, that the synthetic limitations in the preparation of discrete oligomers can be overcome by applying supramolecular coordination chemistry.<sup>[23]</sup>

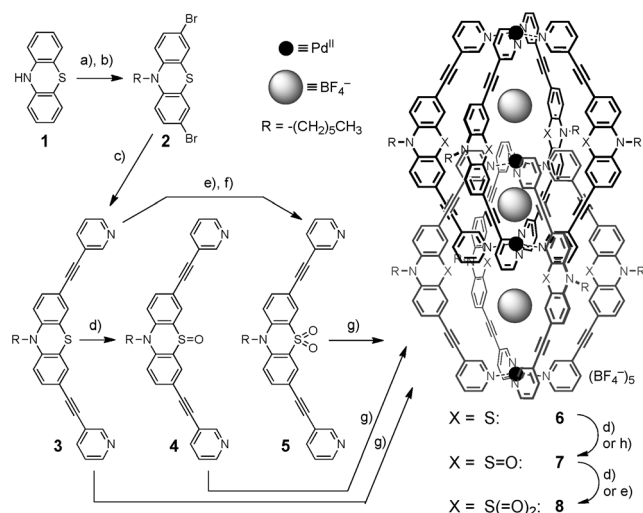
Here, we report the spontaneous and quantitative clustering of eight phenothiazine units into an interpenetrated double cage by self-assembly as well as its eightfold mono- and dioxygenation. The design is based on our previously reported interpenetrated double cages comprising dibenzosuberone backbones and square-planar-coordinated Pd<sup>II</sup> ions.<sup>[24,25]</sup> Our current and previous work, as well as the benzophenone-based interpenetrated double cage reported by Kuroda and co-workers<sup>[26]</sup> show that the [Pd<sub>4</sub>L<sub>8</sub>] design principle tolerates the incorporation of a variety of backbone structures, including the electrochemically interesting compound phenothiazine.

Ligand **3** was synthesized in three steps starting from commercially available 10*H*-phenothiazine (**1**) by *N* alkylation with *n*-hexylbromide, a subsequent selective bromination at the 3,7-positions to give compound **2**,<sup>[19a]</sup> followed by Sonogashira cross-coupling with 2 equiv of 3-ethynylpyridine (Scheme 1). Heating a 2:1 mixture of ligand **3** and [Pd(CH<sub>3</sub>CN)<sub>4</sub>](BF<sub>4</sub>)<sub>2</sub> at 70 °C for 6 h in acetonitrile resulted in the quantitative formation of the interpenetrated coordination compound **6**, as confirmed by <sup>1</sup>H NMR spectroscopy (Figure 1a) and high-resolution ESI mass spectrometry (Figure 2a). Upon conversion of ligand **3** into the highly symmetric double cage **6**, all the <sup>1</sup>H NMR signals split into two sets of equal intensity, in full accordance with our previous findings with the dibenzosuberone-based systems.<sup>[24,25]</sup> The <sup>1</sup>H NMR signals of the pyridine moiety undergo a considerable downfield shift, which indicates the binding to the palladium(II) cations. The signals of the phenothiazine backbone protons and the *N*-CH<sub>2</sub> group of the hexyl residue show an upfield shift upon cage formation

[\*] M. Frank, J. Hey, I. Balcioglu, Prof. Dr. D. Stalke, Prof. Dr. G. H. Clever  
Institute for Inorganic Chemistry  
Georg-August University Göttingen  
Tammannstrasse 4, 37077 Göttingen (Germany)  
E-mail: gclever@gwdg.de  
Homepage: <http://www.clever-lab.de>  
Dr. H. Frauendorf  
Institute for Organic and Biomolecular Chemistry  
Georg-August University Göttingen  
Tammannstrasse 2, 37077 Göttingen (Germany)  
Dr. Y.-S. Chen  
Center for Advanced Radiation Source (ChemMatCARS)  
The University of Chicago c/o APS/ANL (USA)  
Prof. Dr. T. Suenobu, Prof. Dr. S. Fukuzumi  
Department of Material and Life Science, Graduate School of Engineering, Osaka University, ALCA, Japan Science and Technology Agency (JST), Suita, Osaka 565-0871 (Japan)  
Prof. Dr. S. Fukuzumi  
Department of Bioinspired Science, Ewha Womans University  
Seoul 120-750 (Korea)

[\*\*] M.F. thanks the Evonik Foundation and J.H. the CaSuS program of Lower Saxony for PhD fellowships. We thank the DFG (CL 489/2-1), the FCI, and the HeKKSaGOn consortium for support, and Dr. M. John for NMR measurements. ChemMatCARS and the Advanced Photon Source are supported by the NSF Department of Energy (NSF/CHE-0822838, DE-AC02-06CH11357).

Supporting information for this article is available on the WWW under <http://dx.doi.org/10.1002/anie.201302536>.



**Scheme 1.** Synthesis and assembly of phenothiazine-based coordination cage **6** and oxidation to cages **7** and **8**. a) *n*-Hexylbromide,  $\text{KOtBu}$ , THF; b)  $\text{Br}_2$ , HOAc; c) 3-ethynylpyridine,  $\text{CuI}$ ,  $[\text{PdCl}_2(\text{PPh}_3)_2]$ ,  $\text{NEt}_3$ ; d)  $\text{Cu}(\text{NO}_3)_2 \cdot 3\text{H}_2\text{O}$ ,  $\text{CH}_2\text{Cl}_2$ , ultrasound; e) *m*-CPBA,  $\text{CH}_2\text{Cl}_2$ ; f) Fe, HOAc; g)  $[\text{Pd}(\text{CH}_3\text{CN})_4](\text{BF}_4)_2$ ,  $\text{CD}_3\text{CN}$ ; h) two months exposure to air.

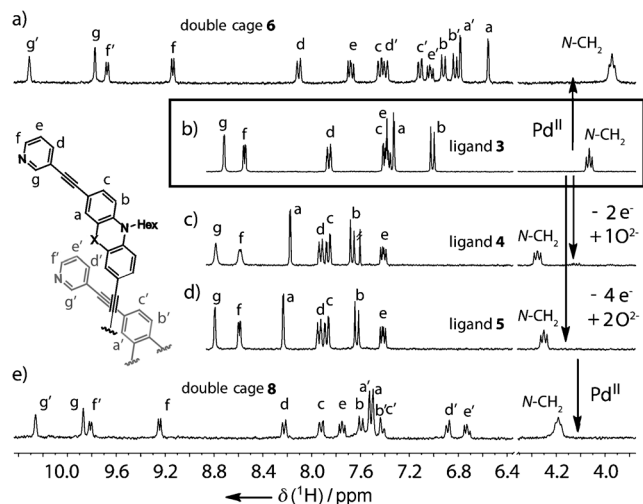


**Figure 1.** a–e)  $^1\text{H}$  NMR spectra (300 MHz,  $\text{CD}_3\text{CN}$ , 293 K) of ligands **3**, **4**, and **5** (2.80 mM) and cages **6** and **8** (0.35 mM; **3**, **6**:  $\text{X} = \text{S}$ ; **4**:  $\text{X} = \text{S}=\text{O}$ ; **5**, **8**:  $\text{X} = \text{S}(\text{=O})_2$ ).

(Figure 1a). The ESI mass spectrum of double cage **6** shows a series of species  $[\text{3BF}_4@\mathbf{6} + n\text{BF}_4]^{(5-n)+}$  ( $n=0-2$ ) containing a variable number of  $\text{BF}_4^-$  counterions (Figure 2a).

Subsequently, we converted ligand **3** into the S-monooxygenated ligand **4** by a two-electron oxidation process with  $\text{Cu}(\text{NO}_3)_2 \cdot 3\text{H}_2\text{O}$  in  $\text{CH}_2\text{Cl}_2$  as a mild oxidizing reagent.<sup>[27]</sup> Compared to **3**, the backbone signals in the  $^1\text{H}$  NMR spectrum of **4** show a significant downfield shift as a result of the oxidation of the sulfur atom (Figure 1c). Like its precursor, sulfoxide **4** can be converted into an interpenetrated double cage **7**. Whereas the ESI mass spectrum confirms a clean and quantitative formation of **7** in solution (Figure 2b), the interpretation of the  $^1\text{H}$  NMR spectra between 238 and 298 K is encumbered by signal broadening.

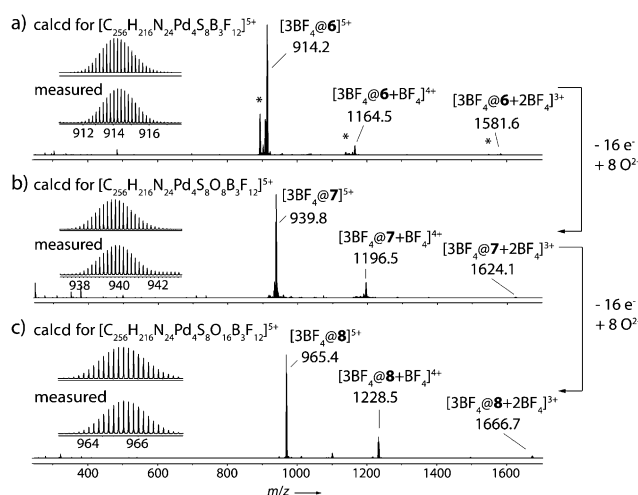


**Figure 2.** ESI mass spectra of the double cages a) **6**, b) **7**, and c) **8** (\* denotes  $\text{Cl}^-$ -containing species  $[\text{2Cl} + \text{BF}_4@\mathbf{6} + n\text{BF}_4]^{(5-n)+}$ ;  $n=0-2$ ).

Nevertheless, the resonances are found in the ppm range expected for a double-cage species (see the Supporting Information). We assume that ligand **4** exists as a quickly equilibrating mixture of two ring-flip isomers with the oxygen substituent in either the favored pseudo-axial or the pseudo-equatorial position<sup>[28]</sup> which leads to a mixture of several diastereomeric double cages upon reaction with  $\text{Pd}^{\text{II}}$ .<sup>[29]</sup>

Next, we performed the oxidation of ligand **3** under harsher conditions by using *meta*-chloroperbenzoic acid (*m*-CPBA) as the oxidizing reagent, which resulted in the formation of an S-dioxygenated derivative with N-oxidized pyridine residues.<sup>[30]</sup> Reductive recovery of the free pyridine rings with iron powder in acetic acid yielded sulfone ligand **5**. The  $^1\text{H}$  NMR spectrum of **5** is similar to that of derivative **4**, with the main difference being a further downfield shift of the proton next to the sulfone group (proton a in Figure 1d) and an upfield shift of its  $\text{N-CH}_2$  proton signal.

Heating a 2:1 mixture of ligand **5** and  $[\text{Pd}(\text{CH}_3\text{CN})_4](\text{BF}_4)_2$  in acetonitrile leads again to the formation of an interpenetrated double cage **8**, as can be rationalized from the ESI mass spectrometric analysis (Figure 2c) and the corresponding  $^1\text{H}$  NMR spectrum (Figure 1e). All proton signals of **8** are relatively sharp, which is similar to the spectrum of nonoxygenated double cage **6**, but different to the spectrum of monooxygenated double cage **7**.

Further characterization of the different ligands and corresponding cages was carried out by UV/Vis and fluorescence spectroscopy (Figure 3). Ligand **3** shows two absorption bands with maxima at 287 nm and 368 nm. The spectra of ligands **4** and **5** are similar to each other (with absorption maxima at 359 nm and 362 nm, respectively), but quite distinct from that of the nonoxidized derivative **3** (Figure 3a). The UV/Vis spectrum of double cage **6** shows two absorptions (Figure 3b) which are shifted to longer wavelengths compared to the spectrum of **3**. Remarkably, the spectrum of double cage **7** shows two intensive absorption maxima, whereas the parental ligand **4** shows only one. The absorption maximum of **8** is only slightly shifted compared to ligand **5**. Nevertheless, both spectra are clearly distinguishable. All

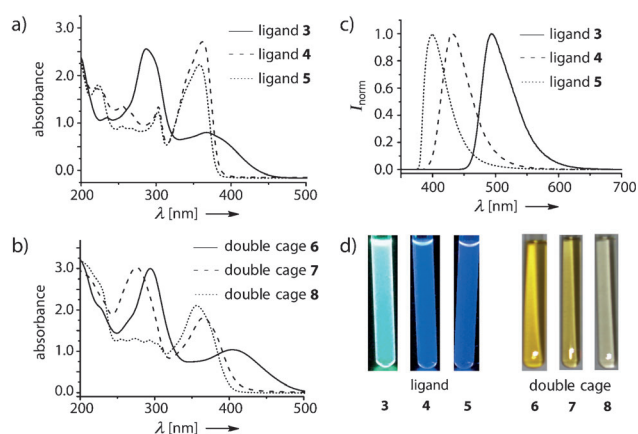


**Figure 3.** a) UV/Vis spectra of ligands **3**, **4**, and **5** (0.35 mm) and b) cages **6**, **7**, and **8** (0.04 mm). c) Fluorescence spectra of ligands **3**, **4**, and **5** (2.80 mm; intensities normalized, excitation at the absorbance maxima). d) Photographs of solutions of the ligands in acetonitrile irradiated at 365 nm (left) and the cages under white light (right).

three ligand derivatives are highly luminescent, as shown by their fluorescence spectra (Figure 3c) and photographs of their solutions in acetonitrile illuminated at 365 nm (Figure 3d). Ligand **3** shows a strong yellow-green fluorescence, while the emissions of **4** and **5** are blue-shifted. In contrast to the ligands, no emission of the corresponding double cages was observed, most probably because of quenching by the metal cations.

Single crystals of nonoxidized double cage **6** suitable for X-ray structure determination were grown by slow diffusion of diethyl ether into a solution of **6** in acetonitrile. The structure reveals that the  $D_4$ -symmetric double cage features three pockets, all filled with a  $\text{BF}_4^-$  ion (Figure 4a). Two further  $\text{BF}_4^-$  ions occupy positions near the outer faces of the two terminal palladium cations and the remaining three  $\text{BF}_4^-$  ions are found in the channels spanning the solid-state structure (see the Supporting Information). The observed double-cage structure is comparable to the structure of the previously reported dibenzosuberone double cage.<sup>[24]</sup>

Surprisingly, we discovered that exposure of the single crystals of compound **6** to air for two months resulted in monooxygenation of all eight phenothiazine backbones to give crystals of compound **7**, presumably in a crystal-to-crystal conversion process (Figure 4b). ESI mass spectrometric analysis of an acetonitrile solution of the crystalline sample of **7** confirmed it had the same molecular composition as the sample obtained starting from ligand **4**.

Although we assume the presence of a mixture of diastereomers in the sample of **7** obtained by solution synthesis starting from ligand **4**, the solid-state-oxidized crystalline sample of **7** consists of only one, highly symmetric isomer, as shown by the X-ray structure determination depicted in Figure 4b. In this structure, all eight phenothiazines carry one oxygen substituent in a pseudo-axial position, thus pointing away from the central  $\text{Pd}_4$  axis. The rotational sense of the oxygen substituents is clockwise in one  $[\text{Pd}_2\text{L}_4]$  subunit and counterclockwise in the other, when viewed along the  $\text{Pd}_4$  axis. Most intriguingly, the molecular structures of **6**

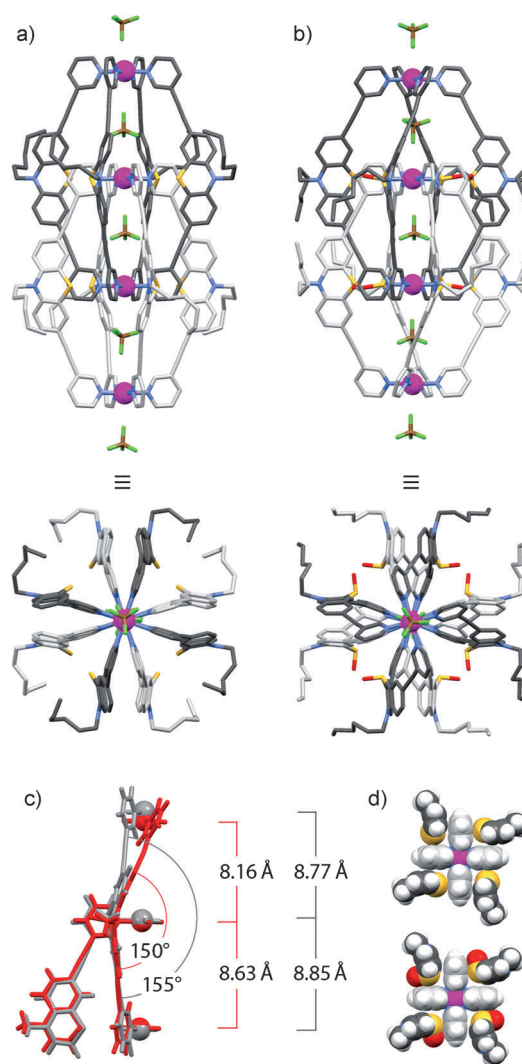


**Figure 4.** X-ray single-crystal structures of double cages a) **6** and b) **7**. c) Partial overlay of structures of **6** (gray) and **7** (red) indicating the changes in the ligand structure and  $\text{Pd-Pd}$  distances. d) Space-filling top view of one of the inner  $\text{Pd}(\text{pyridine})_4$  planes of **6** (top) and **7** (bottom). (C: gray, N: blue, O: red, S: yellow, B: brown, F: green, Pd: purple.)

and **7** are quite distinct from each other. The ring fold of the phenothiazine system (angle between the two benzene ring planes) decreases from  $155^\circ$  to  $150^\circ$  upon monooxygenation, which results in a 5% decrease in the  $\text{Pd-Pd}$  distance in the  $[\text{Pd}_2\text{L}_4]$  subunits (from 17.62 Å in  $[\text{Pd}_2\text{L}_4]$  to 16.79 Å in  $[\text{Pd}_2\text{L}_4]$ ; Figure 4c). In the context of the interpenetrated double-cage structure, this shrinking particularly affects the outer pockets, with the distance between the inner and the neighboring outer  $\text{Pd}$  cation decreasing by 7% from 8.77 Å in **6** to 8.16 Å in **7** (Figure 4c). It is further interesting to compare the position of the interpenetrating ligand backbones near the plane of the inner  $\text{Pd}(\text{pyridine})_4$  complexes (Figure 4d). In both structures, the four pyridine rings are almost perpendicular to the square-planar  $\text{Pd}(\text{N})_4$  coordination sphere. The space-filling top view shows that the phenothiazine moieties of the interdigitated ligands pass through the gaps between the pyridine rings. In both cases, the sulfur atoms point towards



a pyridine ring (distance between the sulfur and the closest ring plane is 3.44 Å in **6** and 3.42 Å in **7**). Since the oxygen substituents on the sulfur atoms in **7** find enough space to occupy the pseudo-axial positions of the phenothiazine systems, the structures of **6** and **7** are surprisingly similar around the inner Pd(pyridine)<sub>4</sub> planes. This must be different for the dioxygenated cage derivative **8**, since every sulfur atom has to accommodate an additional oxygen substituent. A DFT geometry optimization of **8** was conducted to support this assumption (see the Supporting Information).

Subsequently, we tried to oxidize double cage **6** by the same pathway as chosen for ligand **4**: by using a suspension of Cu(NO<sub>3</sub>)<sub>2</sub>·3H<sub>2</sub>O in CH<sub>2</sub>Cl<sub>2</sub>. Monitoring the oxidation process by ESI mass spectrometry revealed a stepwise oxidation, thereby resulting in the formation of **7** as its nitrate salt after a reaction time of about 2 h. The oxidation does not stop at the eightfold monooxygenated product **7**, but proceeds further to yield double cages carrying up to 16 oxygen substituents (**8**; see the Supporting Information).

The nontrivial signal patterns observed in the ESI mass spectra of these reactions (cooperative formation of **7** and further oxygenation to **8** in double steps; see the Supporting Information) indicate that the processes most likely follow a mechanism that strongly depends on the structural and electronic communication between the eight phenothiazine units within the densely packed double-cage architecture. To gain more insight into the different redox behavior of ligand **3** compared to double cage **6**, we first titrated their acetonitrile solutions with the oxidant [Fe<sup>III</sup>(bipyridine)<sub>3</sub>]<sup>3+</sup> to generate the radical cations [3]<sup>•+</sup> and [6]<sup>8•+</sup>, respectively, followed by the reaction with water. As shown in Figure 5, [6]<sup>8•+</sup> hydroly-

of an intramolecular disproportionation pathway. The use of H<sub>2</sub><sup>18</sup>O confirmed water as the oxygen source (see the Supporting Information).

Herein, we reported a series of three highly symmetric, interpenetrated coordination cages based on phenothiazine and its oxidation products. All cages were synthesized by quantitative, metal-mediated self-assembly from the respective ligands. Furthermore, we could show that the oxygenated cage derivatives **7** and **8** are also accessible by direct oxidation of the parental cage **6** in the presence of water. In comparison to ligand **3**, the hydrolysis kinetics of the oxidized species [6]<sup>8•+</sup> suggest a communication of the redox centers within the double cage which results in an accelerated intramolecular disproportionation. We believe that this simple self-assembly strategy for the clustering of redox-active compounds will influence the development of novel functional materials with applications in charge transport and storage. Currently we are further elucidating the spectroscopic and electrochemical properties in the presence and absence of water, as well as the anion-binding capabilities of this new family of interpenetrated coordination cages.

## Experimental Section

The synthesis of ligands **3**, **4**, and **5** from 3,7-dibromo-*N*-hexylphenothiazine (**2**) is described in the Supporting Information. Cages **6**, **7**, and **8** were obtained from the respective ligands by addition of 0.5 equiv of [Pd(CH<sub>3</sub>CN)<sub>4</sub>](BF<sub>4</sub>)<sub>2</sub> in acetonitrile. The oxidation of cage **6** was performed using Cu(NO<sub>3</sub>)<sub>2</sub>·3H<sub>2</sub>O in CH<sub>2</sub>Cl<sub>2</sub> or [Fe<sup>III</sup>(bipyridine)<sub>3</sub>](PF<sub>6</sub>)<sub>3</sub> in CD<sub>3</sub>CN. Single crystals suitable for X-ray crystal-structure analysis were grown by slow diffusion of diethyl ether into a solution of **6** in acetonitrile. The crystals of **7** were obtained by exposure of a sample of **6** to air for two months. CCDC 904004 and 904005 contain the supplementary crystallographic data for this paper. These data can be obtained free of charge from The Cambridge Crystallographic Data Centre via [www.ccdc.cam.ac.uk/data\\_request/cif](http://www.ccdc.cam.ac.uk/data_request/cif).

Received: March 26, 2013

Published online: July 23, 2013

**Keywords:** cage compounds · interpenetration · phenothiazines · redox chemistry · supramolecular chemistry

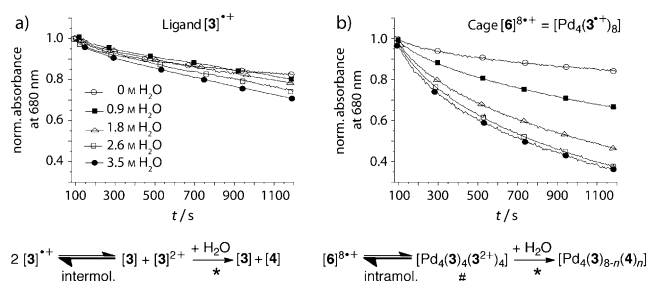


**Figure 5.** Temporal evolution of the radical cation absorption band at 680 nm of a) [3]<sup>•+</sup> and b) [6]<sup>8•+</sup> in the presence of different amounts of water, and proposed mechanisms explaining the observed rate differences (298 K, N<sub>2</sub> atmosphere, concentration: 0.08 mM with respect to **3**, solvent: acetonitrile, oxidant: [Fe<sup>III</sup>(bipyridine)<sub>3</sub>](PF<sub>6</sub>)<sub>3</sub>, oxidant addition at *t* = 0 s, water addition at *t* = 100 s; \*presumably paralleled by further radical decay pathways, # formal fourfold intramolecular disproportionation product).

yses much faster than [3]<sup>•+</sup>, a fact that we assign to the possibility of an intramolecular, hence faster, disproportionation pathway to give phenothiazine dication, which are known intermediates in the reaction with water to give phenothiazine-5-oxide.<sup>[15]</sup> Furthermore, ESI mass spectrometric examination of the hydrolysis products [Pd<sub>4</sub>(**3**)<sub>8-n</sub>(**4**)<sub>n</sub>] (0 ≤ *n* ≤ 8) showed a deviation of the signal pattern from the statistical expectation, which further supports the prevalence

- [1] a) M. Fujita, K. Umemoto, M. Yoshizawa, N. Fujita, T. Kusukawa, K. Biradha, *Chem. Commun.* **2001**, 509; b) S. J. Dalgarno, N. P. Power, J. L. Atwood, *Coord. Chem. Rev.* **2008**, 252, 825; c) D. Tranchemontagne, Z. Ni, M. O'Keeffe, O. Yaghi, *Angew. Chem.* **2008**, 120, 5214; *Angew. Chem. Int. Ed.* **2008**, 47, 5136; d) R. Chakrabarty, P. S. Mukherjee, P. J. Stang, *Chem. Rev.* **2011**, 111, 6810; e) T. K. Ronson, S. Zarra, S. P. Black, J. R. Nitschke, *Chem. Commun.* **2013**, 49, 2476.
- [2] G. H. Clever in *Molecules at Work* (Ed.: B. Pignataro), Wiley-VCH, Weinheim, **2012**.
- [3] a) J. L. Sessler, P. Gale, W.-S. Cho, S. J. Rowan, *Anion Receptor Chemistry* (Monographs in Supramolecular Chemistry), Royal Society of Chemistry, **2006**; b) R. Custelcean, J. Bosano, P. V. Bonnesen, V. Kertesz, B. P. Hay, *Angew. Chem.* **2009**, 121, 4085; *Angew. Chem. Int. Ed.* **2009**, 48, 4025; c) S. O. Kang, J. M. Llinares, V. W. Day, K. Bowman-James, *Chem. Soc. Rev.* **2010**, 39, 3980; d) M. Wang, V. Vajpayee, S. Shanmugaraju, Y.-R. Zheng, Z. Zhao, H. Kim, P. S. Mukherjee, K.-W. Chi, P. J. Stang,

- Inorg. Chem.* **2011**, *50*, 1506; e) J. A. Thomas, *Dalton Trans.* **2011**, 40, 12005; f) G. H. Clever, W. Kawamura, M. Shionoya, *Inorg. Chem.* **2011**, *50*, 4689; g) G. H. Clever, W. Kawamura, S. Tashiro, M. Shiro, M. Shionoya, *Angew. Chem.* **2012**, *124*, 2660; *Angew. Chem. Int. Ed.* **2012**, *51*, 2606.
- [4] P. Mal, B. Breiner, K. Rissanen, J. R. Nitschke, *Science* **2009**, *324*, 1697.
- [5] a) P. Mal, D. Schultz, K. Beyeh, K. Rissanen, J. R. Nitschke, *Angew. Chem.* **2008**, *120*, 8421; *Angew. Chem. Int. Ed.* **2008**, *47*, 8297; b) F. Schmitt, J. Freudenreich, N. P. E. Barry, L. Juillerat-Jeanneret, G. Süß-Fink, B. Therrien, *J. Am. Chem. Soc.* **2012**, *134*, 754; c) Z. Ma, B. Moulton, *Coord. Chem. Rev.* **2011**, *255*, 1623; d) J. E. M. Lewis, E. L. Gavey, S. A. Cameron, J. D. Crowley, *Chem. Sci.* **2012**, *3*, 778.
- [6] a) M. Ziegler, J. Brumaghim, K. Raymond, *Angew. Chem.* **2000**, *112*, 4285; *Angew. Chem. Int. Ed.* **2000**, *39*, 4119; b) D. Fiedler, R. G. Bergman, K. N. Raymond, *Angew. Chem.* **2006**, *118*, 759; *Angew. Chem. Int. Ed.* **2006**, *45*, 745; c) M. Kawano, Y. Kobayashi, T. Ozeki, M. Fujita, *J. Am. Chem. Soc.* **2006**, *128*, 6558; d) C.-Y. Gao, L. Zhao, M.-X. Wang, *J. Am. Chem. Soc.* **2012**, *134*, 824.
- [7] a) D. Vriezema, M. Aragonés, J. Elemans, J. Cornelissen, A. Rowan, R. Nolte, *Chem. Rev.* **2005**, *105*, 1445; b) M. Yoshizawa, J. K. Klosterman, M. Fujita, *Angew. Chem.* **2009**, *121*, 3470; *Angew. Chem. Int. Ed.* **2009**, *48*, 3418; c) *Molecular Encapsulation: Organic Reactions in Constrained Systems* (Eds.: U. H. Brinker, J. Mieusset), Wiley, Hoboken, **2010**; d) M. J. Wiester, P. A. Ulmann, C. A. Mirkin, *Angew. Chem.* **2011**, *123*, 118; *Angew. Chem. Int. Ed.* **2011**, *50*, 114.
- [8] a) J. K. Klosterman, M. Iwamura, T. Tahara, M. Fujita, *J. Am. Chem. Soc.* **2009**, *131*, 9478; b) M. Han, R. Michel, B. He, Y.-S. Chen, D. Stalke, M. John, G. H. Clever, *Angew. Chem.* **2013**, *125*, 1358; *Angew. Chem. Int. Ed.* **2013**, *52*, 1319.
- [9] a) T. Hasobe, *Phys. Chem. Chem. Phys.* **2010**, *12*, 44; b) P. A. Troshin, N. S. Saricic in *Supramolecular Chemistry—From Molecules to Nanomaterials* (Eds.: P. A. Gale, J. W. Steed), Wiley, Chichester, UK, **2012**.
- [10] R. L. Carroll, C. B. Gorman, *Angew. Chem.* **2002**, *114*, 4556; *Angew. Chem. Int. Ed.* **2002**, *41*, 4378.
- [11] S. Bivaud, J.-Y. Balandier, M. Chas, M. Allain, S. Goeb, M. Sallé, *J. Am. Chem. Soc.* **2012**, *134*, 11968.
- [12] G. A. Ozin, A. C. Arsenault, L. Cademartiri, *Nanochemistry: a Chemical Approach to Nanomaterials*, RSC, London, **2009**.
- [13] M. J. Ohlow, B. Moosmann, *Drug Discovery Today* **2011**, *16*, 119.
- [14] T. Manju, N. Manoj, A. M. Braun, E. Oliveros, *Photochem. Photobiol. Sci.* **2012**, *11*, 1744.
- [15] E. E. Bancroft, J. E. Pemberton, H. N. Blount, *J. Phys. Chem.* **1980**, *84*, 2557.
- [16] a) D. G. McCafferty, D. A. Friesen, E. Danielson, C. G. Wall, M. J. Saderholm, B. W. Erickson, T. J. Meyer, *Proc. Natl. Acad. Sci. USA* **1996**, *93*, 8200; b) M. Borgström, O. Johansson, R. Lomoth, H. B. Baudin, S. Wallin, L. Sun, B. Akermark, L. Hammarström, *Inorg. Chem.* **2003**, *42*, 5173; c) E. A. Weiss, M. J. Ahrens, L. E. Sinks, A. V. Gusev, M. A. Ratner, M. R. Wasielewski, *J. Am. Chem. Soc.* **2004**, *126*, 5577; d) H. Tian, X. Yang, R. Chen, Y. Pan, L. Li, A. Hagfeldt, L. Sun, *Chem. Commun.* **2007**, 3741; e) K. Kawai, Y. Osakada, M. Fujitsuka, T. Majima, *J. Phys. Chem. B* **2008**, *112*, 2144; f) M. Marszalek, S. Nagane, A. Ichake, R. Humphry-Baker, V. Paul, S. M. Zakeeruddin, M. Grätzel, *J. Mater. Chem.* **2012**, *22*, 889; g) P. K. Poddutoori, A. S. D. Sandanayaka, N. Zarrabi, T. Hasobe, O. Ito, A. van der Est, *J. Phys. Chem. A* **2011**, *115*, 709.
- [17] V. Balzani, M. Clemente-Leon, A. Credi, B. Ferrer, M. Venturi, A. H. Flood, J. F. Stoddart, *Proc. Natl. Acad. Sci. USA* **2006**, *103*, 1178.
- [18] a) C. Buhrmester, L. Moshurchak, R. L. Wang, J. R. Dahn, *J. Electrochem. Soc.* **2006**, *153*, A288; b) *Lithium-Ion Batteries: Advanced Materials and Technologies* (Eds.: X. Yuan, H. Liu, J. Zhang), CRC, Boca Raton, **2011**.
- [19] a) C. S. Krämer, T. J. J. Müller, *Eur. J. Org. Chem.* **2003**, 3534; b) M. Hauck, J. Schönhaber, A. J. Zuccherro, K. I. Hardcastle, T. J. J. Müller, U. H. F. Bunz, *J. Org. Chem.* **2007**, *72*, 6714; c) M. Sailer, A. W. Franz, T. J. J. Müller, *Chem. Eur. J.* **2008**, *14*, 2602.
- [20] K. Memminger, T. Oeser, T. J. J. Müller, *Org. Lett.* **2008**, *10*, 2797.
- [21] For another example of oligophenothiazines, see T. Okamoto, M. Kuratsu, M. Kozaki, K. Hirotsu, A. Ichimura, T. Matsushita, K. Okada, *Org. Lett.* **2004**, *6*, 3493; for another example of a metal-mediated ring compound based on phenothiazine, see D. Li, X. Tian, G. Hu, Q. Zhang, P. Wang, P. Sun, H. Zhou, X. Meng, J. Yang, J. Wu, B. Jin, S. Zhang, X. Tao, Y. Tian, *Inorg. Chem.* **2011**, *50*, 7997.
- [22] a) J. E. Beves, B. A. Blight, C. J. Campbell, D. A. Leigh, R. T. McBurney, *Angew. Chem.* **2011**, *123*, 9428; *Angew. Chem. Int. Ed.* **2011**, *50*, 9260; b) R. S. Forgan, J.-P. Sauvage, J. F. Stoddart, *Chem. Rev.* **2011**, *111*, 5434; c) J.-F. Ayme, J. E. Beves, C. J. Campbell, D. A. Leigh, *Chem. Soc. Rev.* **2013**, *42*, 1700; d) D. M. Engelhard, S. Freye, K. Grohe, M. John, G. H. Clever, *Angew. Chem.* **2012**, *124*, 4828; *Angew. Chem. Int. Ed.* **2012**, *51*, 4747.
- [23] a) J. W. Steed, J. L. Atwood, *Supramolecular Chemistry*, Wiley, Hoboken, **2009**; b) H.-J. Schneider, *Angew. Chem.* **2009**, *121*, 3982; *Angew. Chem. Int. Ed.* **2009**, *48*, 3924.
- [24] a) S. Freye, J. Hey, A. Torras Galán, D. Stalke, R. Herbst-Irmer, M. John, G. H. Clever, *Angew. Chem.* **2012**, *124*, 2233; *Angew. Chem. Int. Ed.* **2012**, *51*, 2191; b) J. M. Dieterich, G. H. Clever, R. A. Mata, *Phys. Chem. Chem. Phys.* **2012**, *14*, 12746.
- [25] S. Freye, R. Michel, D. Stalke, M. Pawliczek, H. Frauendorf, G. H. Clever, *J. Am. Chem. Soc.* **2013**, *135*, 8476.
- [26] a) M. Fukuda, R. Sekiya, R. Kuroda, *Angew. Chem.* **2008**, *120*, 718; *Angew. Chem. Int. Ed.* **2008**, *47*, 706; b) R. Sekiya, M. Fukuda, R. Kuroda, *J. Am. Chem. Soc.* **2012**, *134*, 10987.
- [27] L. Găină, A. Csámpai, G. Túrós, T. Lovász, V. Zsoldos-Mády, I. A. Silberg, P. Sohár, *Org. Biomol. Chem.* **2006**, *4*, 4375.
- [28] Q. Wang, L. Yang, Z. Xu, Y. Sun, *Acta Crystallogr. Sect. E* **2009**, *65*, o1978.
- [29] Gas-phase DTF calculations (B3LYP/6-311++G(d,p)) of 10-methyl-10H-phenothiazine-5-oxide yield a 2 kJ mol<sup>-1</sup> energetic difference between the pseudo-axial and -equatorial isomers, and a 22 kJ mol<sup>-1</sup> ring-flip barrier.
- [30] T. Ishihara, H. Kakuta, H. Moritani, T. Ugawa, I. Yanagisawa, *Chem. Pharm. Bull.* **2004**, *52*, 1204.